IJMMM International Journal of Minerals, Metallurgy and Materials 矿物冶金与材料学报（英文版）

Effects of heat treatments on microstructures of TiAl alloys

Wen Yu, Jianxin Zhou, Yajun Yin, Zhixin Tu, Xin Feng, Hai Nan, Junpin Lin, and Xianfei Ding

Cite this article as:
Wen Yu, Jianxin Zhou, Yajun Yin, Zhixin Tu, Xin Feng, Hai Nan, Junpin Lin, and Xianfei Ding, Effects of heat treatments on microstructures of TiAl alloys, *Int. J. Miner. Metall. Mater.*, 29(2022), No. 6, pp. 1225-1230. https://doi.org/10.1007/s12613-021-2252-z

---

International Journal of Minerals, Metallurgy and Materials
Volume 29, Number 6, June 2022, Page 1225
https://doi.org/10.1007/s12613-021-2252-z

Effects of heat treatments on microstructures of TiAl alloys

Wen Yu[1,2], *Jianxin Zhou*[1)✉], *Yajun Yin*[1)], *Zhixin Tu*[1)], *Xin Feng*[2,3,4)], *Hai Nan*[2,3,4)], *Junpin Lin*[5)], *and Xianfei Ding*[2,3,4)✉]

1) State Key Laboratory of Materials Processing and Die and Mould Technology, Huazhong University of Science and Technology, Wuhan 430074, China
2) Cast Titanium Alloy R&D Center, Beijing Institute of Aeronautical Materials, Beijing 100095, China
3) Beijing Engineering Research Center of Advanced Titanium Alloy Precision Forming Technology, Beijing 100095, China
4) Beijing Institute of Aeronautical Materials Co., Ltd., Beijing 100094, China
5) State Key Laboratory for Advanced Metals and Materials, University of Science and Technology Beijing, Beijing 100083, China
(Received: 24 November 2020; revised: 6 January 2021; accepted: 15 January 2021)

Abstract: This study aims to investigate the effects of heat treatments on the microstructure of γ-TiAl alloys. Two Ti–47Al–2Cr–2Nb alloy ingots were manufactured by casting method and then heat-treated in two types of heat treatments. Their microstructures were studied by both optical and scanning electron microscopies. The chemical compositions of two ingots were determined as well. The ingot with lower Al content only obtains lamellar structures while the one higher in Al content obtains nearly lamellar and duplex structures after heat treatment within 1270 to 1185°C. A small amount of B2 phase is found to be precipitated in both as-cast and heat-treated microstructures. They are distributed at grain boundaries when holding at a higher temperature, such as 1260°C. However, B2 phase is precipitated at grain boundaries and in colony interiors simultaneously after heat treatments happened at 1185°C. Furthermore, the effects of heat treatments on grain refinement and other microstructural parameters are discussed.

Keywords: TiAl alloys; microstructure; heat treatment; casting

1. Introduction

The titanium aluminides (TiAl), especially γ-based TiAl alloys, are attracting attention as new high-temperature structure materials in the automotive and aerospace industry. This is related to their promising properties, such as excellent oxidation and corrosion resistance, high specific strength and stiffness, low density, good high-temperature stability, and creep resistance [1–4]. As second-generation γ-based TiAl alloy, Ti–48Al–2Cr–2Nb (at%) alloy, referred to as the 4822 alloy, has been successfully implemented and used in the commercial GEnx-1B engines as low-pressure turbine (LPT) blades since 2012 [5–6]. In this paper, the unit of alloy composition is in atom percentage without any special explanation. Ti–47Al–2Cr–2Nb alloy, referred to as the 4722 alloy, is developed based on 4822 alloy to have a higher strength by reducing Al content. However, the deformability is poor because of its natural brittleness induced by the coarse casting structure and segregation in the microstructure immediately after solidification [7–8]. In this case, post processing like heat treatment (HT) must be adopted to overcome this issue.

The method of casting is used to fabricate TiAl alloy components. Such method has advantages not only with low cost but also with more complicated shape. Especially, investment casting is one of the effective ways for manufacturing near-net forming parts of TiAl alloys. 4822 alloy is mainly manufactured in a complex shape through a casting. However, microstructural heterogeneities (such as strong texture and segregation) are known to occur in cast TiAl alloys. Therefore, different HTs have been used to obtain a microstructure with good strength and room temperature ductility during last decades. General Electric (GE) company has studied the relationship between HTs and microstructures in TiAl alloys. Firstly, Kelly *et al.* [9] published a method of processing of γ-TiAl alloy using a HT prior to deformation processing in 1997. It is a three-step HT, including a pre-hot isostatically pressing (HIP) HT, a HIP, and a post-HIP HT. Then, Kelly *et al.* [10–11] published another two methods for processing TiAl alloys in 2001 and 2013. In the new methods, only two-step HT including a HIP cycle and a HT cycle are needed. The pre-HIP HT in the first method is a pretreatment to stabilize the metastable microstructure of the γ-TiAl alloys. And the HIP and post-HIP HT in all three patents are used to eliminate internal voids and micro-porosity in the castings, and obtain an appropriate microstructure respectively. TiAl alloys processed in these three manners preferably exhibit a duplex (DP) microstructure containing equiaxed and lamellar morphologies. In 2015, Guillaume *et al.* [12] from SNECMA company published a method for the treatment of an alloy based on titanium aluminide. The

✉ Corresponding authors: Jianxin Zhou E-mail: zhoujianxin@hust.edu.cn; Xianfei Ding E-mail: xianfeimail@gmail.com

method needs only single-step HT to obtain the final microstructure. No HIP is carried out. Likewise, a DP microstructure is obtained in the alloy after the HT. Furthermore, some researchers have also showed the effect of multistep HTs on microstructure of 4822 alloy or other γ-based TiAl alloys. Harding and Jones [13] has obtained a near gamma (NG) microstructure with only 6vol% of lamellar colonies in Ti–47.9Al–2.0Cr–1.9Nb alloy through a three-step HT like the previous method of GE company. However, a nearly lamellar (NL) microstructure with an average lamellar volume fraction of approximately 95% is formed in Ti–46.67Al–1.95Cr–1.93Nb alloy through a way nearly same as Harding's [14]. Biamino *et al.* [15] have obtained a DP microstructure in the additive manufacturing (AM) 4822 alloy with the composition of Ti–48.14Al–1.65Cr–2.13Nb through a two-step HT like the latter method of GE company. Moreover, some researchers [16–17] have emphasized the specific effect of HT, in particular, upper cycle temperature, heating and cooling rates, and number of cycles on the grain refinement [18–23]. Some studies have also concentrated on massive phase transformations for the grain refinement [24–25]. From the research results above, we find that different microstructures can be formed in 4822 alloy through a nearly same or similar HT regime. It can be explained in two ways: (1) the different original microstructures by different manufacturing methods; (2) changes of alloy element content, especially Al. Among fabrication processes of TiAl alloys, such as casting or AM, it is inevitable to suffer Al loss at different degree in TiAl parts caused by evaporation due to its higher vapor pressure, compared with other metallic elements [26]. For 4822 alloy, the as-cast microstructure is usually fully lamellar (FL) structure. In this way, extremely slight changes for Al content in TiAl alloys will have an obvious effect on the phase transus, which may influence the microstructure after HT. However, no studies have reported about the differences of microstructure and HT in TiAl alloys due to Al content changes.

In this paper, two 4722 alloy ingots with different Al contents are used to study the effects of HTs on the microstructures. Changes of microstructure of the alloys in different HT conditions are systematically studied. This study can provide some reference information on the composition control and subsequent HT of TiAl alloys.

2. Experimental

Two TiAl ingots with the nominal composition of Ti–47Al–2Cr–2Nb, were prepared by first vacuum arc re-melting, then vacuum induction re-melting, finally vacuum arc re-melting, and pouring into an Y_2O_3 coated ceramic molds preheated to 800°C. The alloy chemistries are summarized in Table 1. They are named as Alloy A and Alloy B respectively according to their different Al contents. Specimens with the size of 20 mm × 16 mm × 10 mm were cut from the two ingots. Subsequent HTs were carried out under air in a muffle furnace. Table 2 lists two types of HT including a two-step HT and a single-step HT. Two-step HT include a 1260°C/4 h HT simulating the HIP process but without applying external pressure and a subsequent HT at temperature within the range of 1290 to 1185°C. Two-step HTs are firstly applied to Alloy A. However, there are only lamellar structures observed in the Alloy A. The HIP process is conducted to consolidate the alloy, and does not affect the microstructural type after the final HT. Therefore, only single-step HTs are applied to Alloy B to investigate why only lamellar structures form in Alloy A after the two-step HTs. All specimens were heated to HT temperatures with a heating rate of 20°C·min^{-1}. After different holding times, these specimens were cooled to room temperature in the furnace (FC). Specimens for microstructural investigations were cut perpendicularly to the longitudinal direction in order to avoid the influence of the oxidized surface layer. The microstructures were characterized by optical microscopy (OM) and scanning electron microscopy (SEM) in back-scattered electron (BSE) mode. OM was used to investigate the microstructure at lower magnification times and measured the size of the lamellar colonies by an intercept method. The different phases present in the microstructure were discriminated based on their contrast on BSE images.

Table 1. Chemical compositions of the experimental alloys in at%

Alloy	Ti	Al	Cr	Nb	O
A	Bal.	46.36	2.01	2.05	0.12
B	Bal.	47.01	2.02	2.09	0.13

Table 2. Types of HT applied to the specimens of two alloys

Alloy	HT
A	1260°C/4 h/FC +1290°C/5 h/FC
	1260°C/4 h/FC + 1270°C/5 h/FC
	1260°C/4 h/FC + 1240°C/5 h/FC
	1260°C/4 h/FC + 1185°C/5 h/FC
	1260°C/4 h/FC
	1185°C/4 h/FC
B	1260°C/4 h/FC
	1185°C/4 h/FC

3. Results

3.1. As-cast microstructures

Fig. 1 shows the OM and BSE microstructures of the as-cast alloys. The as-cast microstructures of both two alloys are FL structures composed of the alternately arranged α_2 and γ phase lamellae. The majority of lamellar colonies exhibit a columnar morphology with an inhomogeneous size. Alloy A contains a mean colony size of 421.51 μm with a mean interlamellar spacing of 1.25 μm, while Alloy B consists of a little coarser colony size of 561.03 μm with a mean interlamellar spacing of 1.54 μm. In addition to the lamellar colonies, there are a few γ grains located along colony boundaries and many punctate and needlelike B2 particles located at grain boundaries, which is predominating, and in colony interiors, as shown by black arrows and white arrows in Fig. 1(c) and (d), respectively. The mean diameter of the γ grains in Alloy A

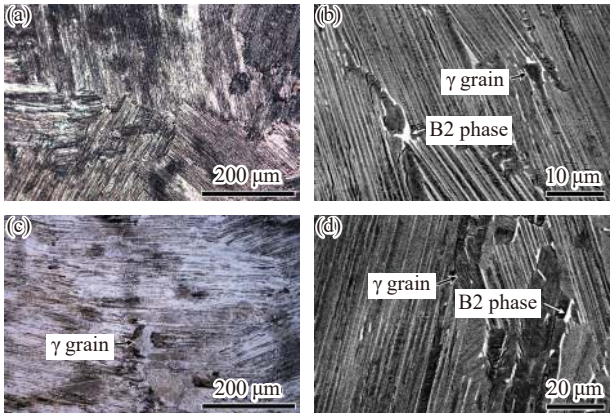

Fig. 1. OM (a, c) and BSE (b, d) images of the as-cast 4722 alloys: (a, b) Alloy A; (c, d) Alloy B.

and Alloy B is approximately 8.14 and 47.87 μm, respectively.

3.2. Heat-treated microstructures

OM images in Fig. 2 show the typical FL structures in Alloy A after two-step HT including the first HT at 1260°C for 4 h which simulates HIP process and a subsequent HT at 1290, 1270, 1240, and 1185°C for 5 h, respectively. It is observed by BSE images in Fig. 2 that lamellar colonies, γ grains (as shown by black arrows) and B2 phase (as shown by white arrows) exist in the microstructures. The γ grains are distributed at several colony boundaries and are not enough

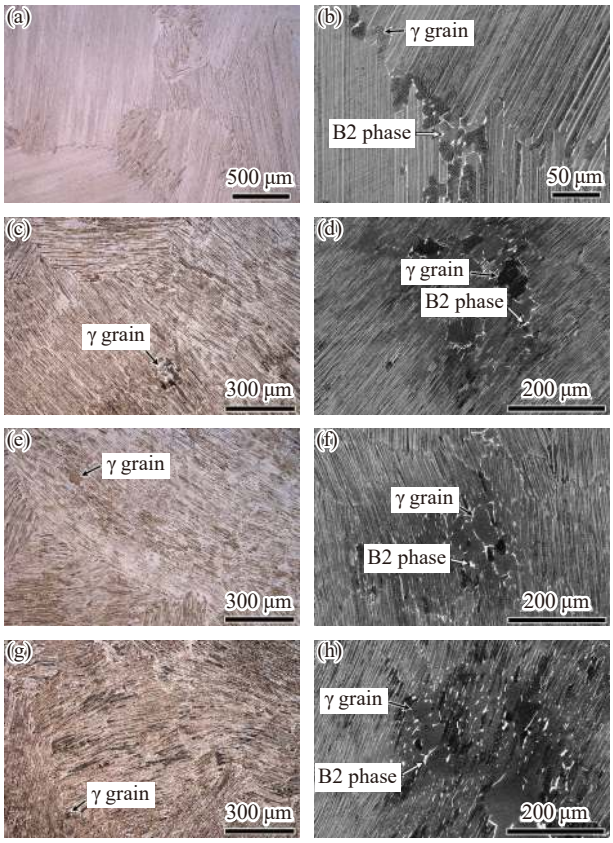

Fig. 2. OM (a, c, e, g) and BSE (b, d, f, h) images of Alloy A after different two-step HTs: (a, b) 1260°C/4 h/FC + 1290°C/5 h/FC; (c, d) 1260°C/4 h/FC + 1270°C/5 h/FC; (e, f) 1260°C/4 h/FC + 1240°C/5 h/FC; (g, h) 1260°C/4 h/FC + 1185°C/5 h/FC.

to form a NL structure. The B2 phase is almost distributed at grain boundaries. And none of B2 phase is observed in colony interiors.

Fig. 3 shows the changes in interlamellar spacing of Alloy A after different two-step HTs by high magnification BSE images. It can be observed that with the temperature decreasing the γ laths are coarsened gradually. As indicated above, no B2 phase is formed in colony interiors. Fig. 4 shows the dependences of the lamellar colony size and interlamellar spacing on holding temperatures in the Alloy A. Excepting the treatment at 1290°C whose colony size is 966.31 μm, treatments at another three lower temperatures can refine lamellar colony size at some degree in comparation with that in as-cast state. The mean colony size can be refined from 421.51 μm in as-cast state to 330.59 μm after treatment at 1270°C. However, when continuing to lower the holding temperature to 1240 and 1185°C, the colony size can not be refined further and remains approximately 330 μm. Besides, the mean interlamellar spacing increases gradually from 1.64 to 3.25 μm with decreasing the holding temperature.

Fig. 5(a) and (c) shows the OM images of Alloy B after single-step HTs at 1260 and 1185°C, respectively. It can be observed that the NL and DP structures composed of γ grains

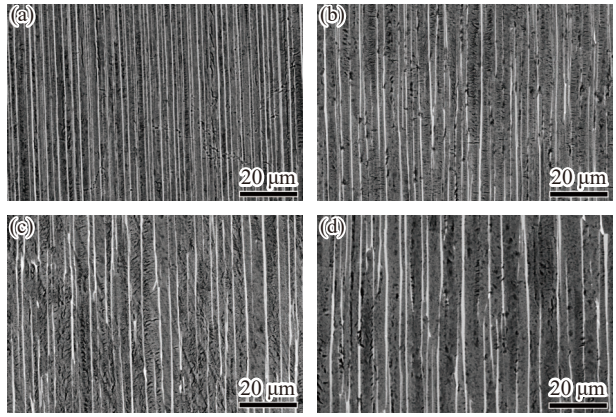

Fig. 3. BSE images of Alloy A at high magnification showing the interlamellar spacing after different two-step HTs: (a) 1260°C/4 h/FC + 1290°C/5 h/FC; (b) 1260°C/4 h/FC + 1270°C/5 h/FC; (c) 1260°C/4 h/FC + 1240°C/5 h/FC; (d) 1260°C/4 h/FC + 1185°C/5 h/FC.

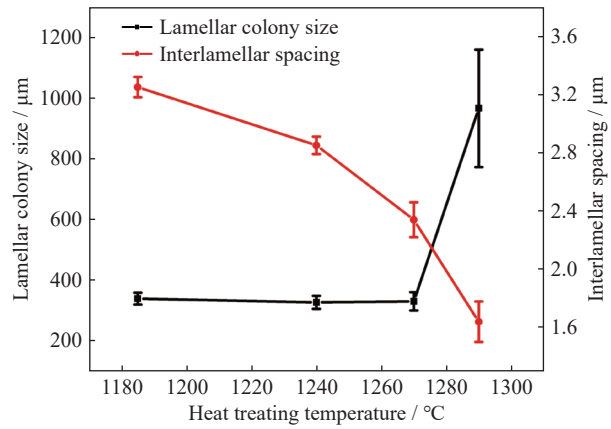

Fig. 4. Dependences of the lamellar colony size and interlamellar spacing on holding temperatures in Alloy A.

and alternating plates of γ and α_2 phases are formed at 1260 and 1185°C, respectively. The γ grains are distributed not only at colony boundaries but also in colony inferiors. BSE images in Fig. 5 indicate that B2 phase (as shown by white arrows) is formed at grain boundaries and in colony inferiors after single-step HTs. However, B2 phase is only located at grain boundaries after HT at 1260°C while located at grain boundaries as well as in colony inferiors after HT at 1185°C. With decreasing the temperature from 1260 to 1185°C, the volume fraction of γ grains increases from 26.16% to 34.11%, and the mean γ grain size stays nearly same about 50 μm.

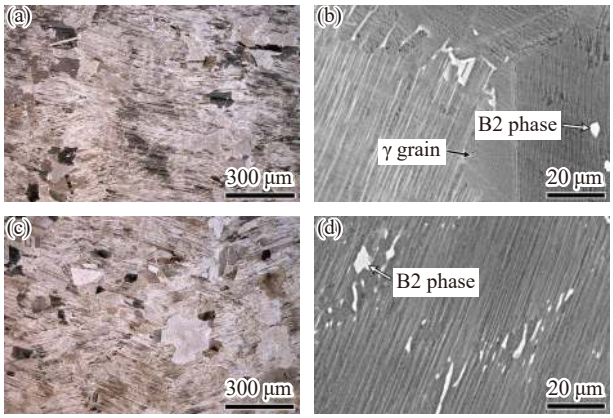

Fig. 5. OM (a, c) and BSE (b, d) images of Alloy B after different single-step HTs: (a, b) 1260°C/4 h/FC; (c, d) 1185°C/4 h/FC.

Fig. 6(a) and (c) shows the OM images of Alloy A after single-step HTs at 1260 and 1185°C, respectively. It can be observed that a FL structure is formed at higher temperature 1260°C while a NL microstructure is formed at lower temperature 1185°C. The γ grains are almost distributed at colony boundaries-with a smaller mean size 24.01 μm and volume fraction 8.45% in the NL microstructure compared with Alloy B heat treated at 1185°C, as described in Fig. 6(c). In addition, B2 phase is observed in NL microstructure to be located at grain boundaries and in colony interiors, Fig. 6(d), just like the distribution in Alloy B after the same treatment.

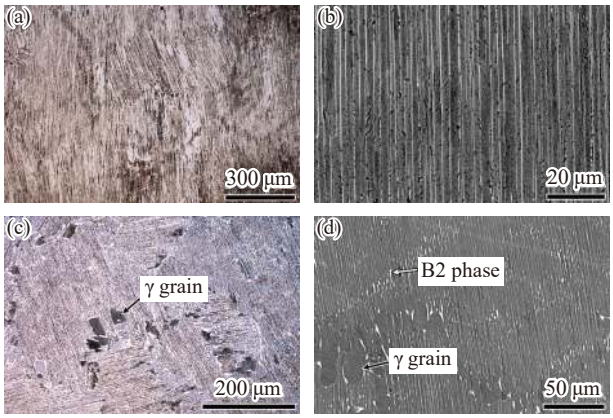

Fig. 6. OM (a, c) and BSE (b, d) images of Alloy A after different single-step HTs: (a, b) 1260°C/4 h/FC; (c, d) 1185°C/4 h/FC.

And after treatment at 1260°C, no B2 phase is found in colony interiors as shown in Fig. 6(b).

4. Discussion

4.1. Effects of Al content on microstructures and HTs

In the two γ-TiAl alloys, small change of Al content can make apparent differences in microstructures. In as-cast microstructures, the mean size of γ grains and interlamellar spacing in Alloy B are bigger than in Alloy A. This can be attributed to that more γ phase is formed in Alloy B with higher Al content than in Alloy A with lower Al content. As indicated above, Alloy A with 46.36at% Al only obtains lamellar structure (FL or NL) after either two-step HTs or single-step HTs, while Alloy B obtains DP structure just after single-step HT at 1185°C. Since it does not make an apparent difference in the microstructural type after two-step HTs and single-step HTs, Fig. 2(c) and (e) and Fig. 6(a), that cannot be attributed to the simulating HIP process. Thus, it must be the Al content that leads to the result.

To simplify the discussion, binary TiAl phase diagram [27] is employed to illustrate the microstructure transformation upon heating and cooling since the accurate Ti–Al–Cr–Nb phase diagram has not been established up to now. And the influence of the elements Cr and Nb is evaluated in the form of Al equivalent generally. The central portion of the Ti–Al binary phase diagram is shown in Fig. 7. The phase boundaries of the pseudo-binary system of the present alloys are estimated and shown with dotted lines based on Al equivalent using the formula $C_{Al,eq} = C_{Al} - 0.3C_{Nb} - 0.1C_{Cr}$, where $C_{Al,eq}$ is the Al equivalent composition, and C_{Al}, C_{Nb}, and C_{Cr} are the Al, Nb, and Cr composition in the alloy, respectively [28–30]. The pseudo-binary phase diagram for the present alloy indicates that the alloying addition of Cr and Nb shifts the phase boundaries distinctly. The α/α+γ boundary is lowered. And the α+γ/γ boundaries are shifted toward the titanium-rich side. The upper portion of the α+γ/γ boundary appears to be shifted toward the Al side. It means that Alloy A and Alloy B will pass single γ phase field as

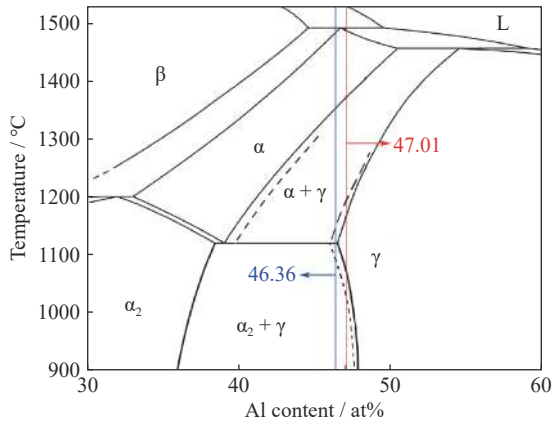

Fig. 7. Central portion of the Ti–Al binary phase diagram and the dotted lined pseudo-binary phase boundaries for the present alloy concerning Al equivalent. L denotes the liquid phase.

shown by blue and red lines respectively, which can influence the microstructure transformation.

When heated in the $\alpha_2+\gamma$ phase field, the microstructure keeps nearly unchanged. With the temperature increasing further into the single γ phase field, γ grains start to nucleate at colony boundaries as well as in colony interiors. Due to the lower Al content, the period through the single γ phase field in Alloy A is much less than in Alloy B at the same heating rate. In this case, γ nuclei in Alloy B, which are formed in the single γ phase field, are much more than in Alloy A. In addition, these γ nuclei are not able to grow further because of the higher heating rate. When the temperature increases into α+γ phase field, the order–disorder transition from α_2 to α occurs. At the holding temperature, α phase including the order–disorder transition and the transformation from γ phase is in equilibrium with γ phase, and the γ nuclei grow simultaneously. Considered the γ nuclei in Alloy B are much more than in Alloy A, more γ nuclei can grow into γ grains in Alloy B. Thus, only a lamellar structure is formed in Alloy A while a DP structure is formed in Alloy B.

For the single-step HTs in Alloy A and Alloy B, apparent changes in phase constitution and distribution, especially for B2 phase, are observed from BSE images in Figs. 5 and 6. When heat treated at higher temperature 1260°C, B2 phase is observed to be only located at colony boundaries. However, when heat treated at lower temperature 1185°C, B2 phase is observed at colony boundaries and in colony interiors simultaneously. Since the diffusion of alloying elements is slow at this lower temperature 1185°C, the B2 phase in as-cast microstructures is retained after the HT. However, for the two-step HTs in Alloy A, no B2 phase is found in colony interiors in Figs. 2 and 3 even if the second step HT has been conducted in various temperatures. That can be attributed to the higher diffusivity of alloying elements at 1260°C. In addition, more Cr and Nb elements (regarded as β stabilizers) are excluded to grain boundaries when more γ grains are formed in DP structure than in NL structure after HTs at 1185°C. Therefore, the volume fraction of B2 phase is more in Alloy B than in Alloy A.

4.2. Effects of HTs on the microstructural parameters

Microstructural parameters in γ-TiAl alloy, such as grain size, interlamellar spacing, phase constitution, and distribution, etc, are in the control of HTs. For the two-step HTs in Alloy A, the colony sizes are 966.31 and 330.59 μm corresponding to the HTs at 1290 and 1270°C, respectively. This must be attributed to that the grain growth of α phase at temperature above α transus is rapid resulting in very large FL grains, Fig. 2(a). The fast diffusivity of elements expected at such high temperature and the absence of second phase are likely to be the main causes to the rapid grain growth. Based on the change in colony size, α transus can be deduced to be between 1290 and 1270°C. When the temperature continued to decrease in the range of 1270 to 1185°C, the colony size remains almost invariable due to a very few γ grains existing in the microstructures shown in Fig. 2(c), (e), and (g). To maintain the phase equilibrium in the microstructure, γ phase is increasing gradually in the way of coarsening γ laths with decreasing the temperature, Fig. 3(b), (c), and (d). Compared with the colony size in as-cast state, the colony size is refined ~20% after HTs at 1185–1270°C. When Alloy A are isothermally held at 1185–1270°C, γ nuclei which nucleate at colony boundaries begin to extend to the adjacent colonies. In this way, the size of some colonies can be shrunk and the mean size of colonies is reduced.

4.3. Effects of original microstructures on heat-treated microstructures

The original microstructure is a crucial factor for modifying the microstructure using HT. In our study, for the lower Al content Alloy A with a FL structure, even if the temperature decreases to 1185°C, no DP structure can be formed. Similar case was found in Mercer's study, in which a cast lamellar Ti–48Al–2Cr–2Nb alloy with 46.67at% Al content obtained a NL structure after HT at 1200°C. However, Huang and Hall indicated that Ti–46Al–2Cr alloy through extrusion obtained a DP structure after HT at 1250°C [31].

Kim has pointed out that microstructures developed from forged two-phase TiAl alloys are virtually unlimited in variations. The microstructures can be conveniently divided into four types, that is, NG, DP, NL, and FL structures [32]. In Kim's study, Ti–47Al–1Cr–1V–2.5Nb alloy forged isothermally at 1180°C resulted in a banded microstructure that consisted of deformed lamellar plates and partially recrystallized fine γ grains with regions containing α_2 fine particles. In such a high energy condition, the microstructure will recrystallize into α grains and γ grains during thermal holding. And if the HTs are conducted at temperatures where the volume fractions of γ phase and α phase are approximately equal, then a DP microstructure will be formed after cooling. Moreover, a typical DP structure is formed in Ti–46Al–1.9Cr–3Nb alloy just after forging at 1200°C without additional HTs [23].

According to the above analyses, it seems to conclude that γ-TiAl alloys can be easily regulate their microstructure into DP or lamellar structure when they are manufactured with an original NG or DP structure, or in a deformed condition. If they are manufactured with an original FL structure with a lower Al content, the lamellar structure will not be destroyed and refined easily.

5. Conclusions

In this paper, the effects of normalizing and annealing processes on the microstructures of cast FL 4722 alloys were studied. The main results can be summarized as follows.

(1) HTs on Ti–46.36Al–2.01Cr–2.05Nb alloy can only obtain FL or NL structures. Holding at 1270°C can refine cast lamellar colony size from 421.51 to 330.59 μm. However, no more refinement is observed when holding temperature decreasing within the range of 1270 to 1185°C.

(2) HTs at 1260 and 1185°C on Ti–47.01Al–2.02Cr–2.09Nb can obtain NL and DP structure, respectively. Decreasing holding temperature from 1260 to 1185°C can in-

crease the volume fraction of γ grains from 26.16% to 34.11%.

(3) Al content and original microstructure in 4722 alloy have a great influence on HTs in controlling the structural type. A DP structure may not be formed in the cast FL 4722 alloy with lower Al content after HTs in the α+γ phase field.

(4) B2 phase can be precipitated only at grain boundaries when holding at higher temperature such as 1260°C. However, the B2 phase precipitation is observed at grain boundaries and in colony interiors simultaneously after HT at 1185°C.

Acknowledgements

This work was financially supported by the National Natural Science Foundation of China (Nos. U1808216, 51671026, and 51671016), the National Key Research and Development Program of China (Nos. 2020YFB1710100 and 2018YFB1106000), the State Key Lab of Advanced Metals and Materials (No. 2019-ZD05), the Beijing Natural Science Foundation (No. 2222092), and the National Science and Technology Major Project (No. J2019-VI-0003-0116).

Conflict of Interest

The authors declare no potential conflict of interest.

References

[1] H. Clemens and S. Mayer, Intermetallic titanium aluminides in aerospace applications—Processing, microstructure and properties, *Mater. High Temp.*, 33(2016), No. 4-5, p. 560.

[2] F. Appel, H. Clemens, and F.D. Fischer, Modeling concepts for intermetallic titanium aluminides, *Prog. Mater. Sci.*, 81(2016), p. 55.

[3] D.M. Dimiduk, Gamma titanium aluminide alloys—An assessment within the competition of aerospace structural materials, *Mater. Sci. Eng. A*, 263(1999), No. 2, p. 281.

[4] Y.W. Kim, Intermetallic alloys based on gamma titanium aluminide, *JOM*, 41(1989), No. 7, p. 24.

[5] Y.W. Kim and S.L. Kim, Advances in gammalloy materials–processes–application technology: Successes, dilemmas, and future, *JOM*, 70(2018), No. 4, p. 553.

[6] B.P. Bewlay, S. Nag, A. Suzuki, and M.J. Weimer, TiAl alloys in commercial aircraft engines, *Mater. High Temp.*, 33(2016), No. 4-5, p. 549.

[7] J.K. Kim, J.H. Kim, J.Y. Kim, S.H. Park, S.W. Kim, M.H. Oh, and S.E. Kim, Producing fine fully lamellar microstructure for cast γ-TiAl without hot working, *Intermetallics*, 120(2020), art. No. 106728.

[8] J. Aguilar, A. Schievenbusch, and O. Kättlitz, Investment casting technology for production of TiAl low pressure turbine blades—Process engineering and parameter analysis, *Intermetallics*, 19(2011), No. 6, p. 757.

[9] T.J. Kelly, C.M. Austin, and R.E. Allen, *Processing of Gamma Titanium–Aluminide alloy Using a Heat Treatment Prior to Deformation Processing*, U.S. Patent, Appl. 08/376519, 1997.

[10] T.J. Kelly, B.P. Bewlay, M.J. Weimer, and R.K. Whitacre, *Methods for Processing Titanium Aluminide Intermetallic Compositions*, European Patent, Appl. 13159885.6, 2013.

[11] T.J. Kelly, M.J. Weimer, C.M. Austin, B. London, D.E. Larson, and D.A. Wheeler, *Heat Treatment of Gamma Titanium Aluminide Alloys*, U.S. Patent, Appl. 08/262168, 2001.

[12] M. Guillaume, M.C. Jeanne, and M.P. Marie, *Heat Treatment of an Alloy Based on Titanium Aluminide*, U.S. Patent, Appl. 15/302418, 2015.

[13] T.S. Harding and J.W. Jones, Fatigue thresholds of cracks resulting from impact damage to γ-TiAl, *Scripta Mater.*, 43(2000), No. 7, p. 623.

[14] C. Mercer, J. Lou, and W.O. Soboyejo, An investigation of fatigue crack growth in a cast lamellar Ti–48Al–2Cr–2Nb alloy, *Mater. Sci. Eng. A*, 284(2000), No. 1-2, p. 235.

[15] S. Biamino, A. Penna, U. Ackelid, S. Sabbadini, O. Tassa, P. Fino, M. Pavese, P. Gennaro, and C. Badini, Electron beam melting of Ti–48Al–2Cr–2Nb alloy: Microstructure and mechanical properties investigation, *Intermetallics*, 19(2011), No. 6, p. 776.

[16] Y. Mine, K. Takashima, and P. Bowen, Effect of lamellar spacing on fatigue crack growth behaviour of a TiAl-based aluminide with lamellar microstructure, *Mater. Sci. Eng. A*, 532(2012), p. 13.

[17] H.L. Zhu, D.Y. Seo, K. Maruyama, and P. Au, Effect of lamellar spacing on microstructural instability and creep behavior of a lamellar TiAl alloy, *Scripta Mater.*, 54(2006), No. 12, p. 1979.

[18] Z.T. Gao, J.R. Yang, Y.L. Wu, R. Hu, S.L. Kim, and Y.W. Kim, A newly generated nearly lamellar microstructure in cast Ti–48Al–2Nb–2Cr alloy for high-temperature strengthening, *Metall. Mater. Trans. A*, 50(2019), No. 12, p. 5839.

[19] M. Ahmadi, S.R. Hosseini, and S.M.M. Hadavi, Effects of heat treatment on microstructural modification of as-cast gamma-TiAl alloy, *J. Mater. Eng. Perform.*, 25(2016), No. 6, p. 2138.

[20] Y.J. Du, J. Shen, Y.L. Xiong, Z. Shang, and H.Z. Fu, Stability of lamellar microstructures in a Ti–48Al–2Nb–2Cr alloy during heat treatment and its application to lamellae alignment as a quasi-seed, *Intermetallics*, 61(2015), p. 80.

[21] A. Szkliniarz, Grain refinement of Ti–48Al–2Cr–2Nb alloy by heat treatment method, *Solid State Phenom.*, 191(2012), p. 221.

[22] A. Kościelna and W. Szkliniarz, Effect of cyclic heat treatment parameters on the grain refinement of Ti–48Al–2Cr–2Nb alloy, *Mater. Charact.*, 60(2009), No. 10, p. 1158.

[23] T. Novoselova, S. Malinov, and W. Sha, Experimental study of the effects of heat treatment on microstructure and grain size of a gamma TiAl alloy, *Intermetallics*, 11(2003), No. 5, p. 491.

[24] J.N. Wang, J. Yang, and Y. Wang, Grain refinement of a Ti–47Al–8Nb–2Cr alloy through heat treatments, *Scripta Mater.*, 52(2005), No. 4, p. 329.

[25] W.J. Zhang, G.L. Chen, and E. Evangelista, Formation of α phase in the massive and feathery γ-TiAl alloys during aging in the single α field, *Metall. Mater. Trans. A*, 30(1999), No. 10, p. 2591.

[26] H.P. Tang, G.Y. Yang, W.P. Jia, W.W. He, S.L. Lu, and M. Qian, Additive manufacturing of a high niobium-containing titanium aluminide alloy by selective electron beam melting, *Mater. Sci. Eng. A*, 636(2015), p. 103.

[27] J.C. Schuster and M. Palm, Reassessment of the binary Aluminum–Titanium phase diagram, *J. Phase Equilib. Diffus.*, 27(2006), No. 3, p. 255.

[28] P. Han, H.C. Kou, J.R. Yang, G. Yang, and J.S. Li, Solidification microstructure characteristics of Ti–44Al–4Nb–2Cr–0.1B alloy under various cooling rates during mushy zone, *Rare Met.*, 35(2016), No. 1, p. 35.

[29] Y. Liu, R. Hu, H.C. Kou, J. Wang, T.B. Zhang, J.S. Li, and J. Zhang, Solidification characteristics of high Nb-containing γ-TiAl-based alloys with different aluminum contents, *Rare Met.*, 34(2015), No. 6, p. 381.

[30] Y. Liu, R. Hu, G. Yang, H.C. Kou, T.B. Zhang, J. Wang, and J.S. Li, Widmannstätten laths in Ti48Al2Cr2Nb alloy by undercooled solidification, *Mater. Charact.*, 107(2015), p. 156.

[31] S.C. Huang and E.L. Hall, The effects of Cr additions to binary TiAl-base alloys, *Metall. Trans. A*, 22(1991), No. 11, p. 2619.

[32] Y.W. Kim, Microstructural evolution and mechanical properties of a forged gamma titanium aluminide alloy, *Acta Metall. Mater.*, 40(1992), No. 6, p. 1121.